Published in Physical Review B 58, issue 8, R4270-R4273, 1998
which should be used for any reference to this work

Observation of the reversible H-induced structural transition in thin Y films via x-ray photoelectron diffraction

J. Hayoz, S. Sarbach, Th. Pillo, E. Boschung, D. Naumović, P. Aebi,
and L. Schlapbach
Institut de Physique, Université de Fribourg, Pérolles, CH-1700 Fribourg, Switzerland

Yttrium can be loaded with hydrogen up to high concentrations causing dramatic structural and electronic changes of the host lattice. We report on the reversibility of hydrogen loading in thin single-crystalline Y films grown by vapor deposition on W(110). Under a H_2 partial pressure of 1×10^{-5} mbar the hexagonal-closed-packed Y films convert to the face-centered-cubic Y dihydride. Unloading is accomplished by annealing the dihydride to 1000 K. No loss of crystallinity is observed during these martensitic transformations of the Y lattice. Moreover, we demonstrate a model to determine the H concentration in Y *in situ*.

The interaction of hydrogen with Y, La, and the rare-earth (RE) metals has been the subject of numerous investigations due to the interesting temperature- and concentration-dependent structures and properties observed in the solid solution (α phase) as well as in the stable dihydride (β) and trihydride (γ) phases.[1] An example is the recent observation of switchable optical properties of Y and La hydride films where shiny, metallic dihydride films become transparent semiconductors in the trihydride phase.[2] It is obvious that the geometrical and electronic structure of RE hydrides are key quantities for the understanding of all these properties.

For Y, the geometrical structure of the host-lattice and the hydrogen atom positions are well known over the entire range of H concentrations: Y crystallizes in the hexagonal-closed-packed (hcp) structure, while its dihydride transforms to a face-centered-cubic (fcc) CaF_2-type structure.[1] The insulating trihydride, finally, possesses a hcp unit cell (HoD_3 type).[3] The electronic structure of Y hydrides, however, is still a matter of dispute.[1]

Up until recently most work on hydrogen in Y has been done using polycrystalline bulk or powder samples. Existing photoemission spectroscopy data therefore only yields information on the occupied density of states or on charge transfer from Y to H via core-level shifts.[4–7] The reason for the absence of experimental band-structure data based on angle-resolved ultraviolet photoemission spectroscopy (ARUPS) is due to the fact that loss of single crystallinity during the first transition (α to β) is difficult to avoid and that most bulk samples decompose into powder while going from β to γ.[1] Recently an x-ray diffraction study demonstrated that in thin, monocrystalline Y films, the structural coherence is maintained during cycling *ex situ* between the dihydride and the trihydride phases.[8]

In this study we demonstrate that it is possible to transform thin, single-crystalline Y films into the dihydride phase and to unload them again without loss of order. We used x-ray photoelectron diffraction (XPD) to observe, in real space and near the surface, the changes occurring due to the H-induced structural transitions. In contrast to the previous study,[8] experiment, loading, and unloading are done *in situ*, and the films are not capped by a protective Pd layer, a most crucial prerequisite for future ARUPS studies on the electronic structure of Y as a function of hydrogen content. Furthermore, based on XPD and hydrogen-induced core-level shifts we propose a model to determine the H concentration in Y *in situ*.

XPD has been chosen because of its chemical sensitivity and its sensitivity to local real-space order. It is a powerful technique for surface structural investigations,[9] and it has been shown that full hemispherical XPD patterns provide very direct information about the near-surface structure.[10–13] At photoelectron kinetic energies above about 500 eV, the strongly anisotropic scattering by the ion cores leads to a forward focusing of the electron flux along the emitter-scatterer axis. The photoelectron angular distribution, therefore, is to a first approximation a forward-projected image of the atomic structure around the photoemitters. The XPD data are presented in so-called diffractograms, i.e., in a stereographic projection and in a linear gray scale with maximum intensity corresponding to white (Fig. 1). The center of each plot corresponds to the surface normal (polar emission angle $\Theta=0°$) while the outer circle represents directions parallel to the surface ($\Theta=90°$). Single-scattering cluster (SSC) calculations have been used to interpret the XPD patterns. The SSC model used for photoelectron diffraction is discussed in detail elsewhere.[9] Note that the cross section for forward scattering increases with increasing atomic number.[14] As a rough guide, at electron kinetic energies above a few hundred eV, forward scattering is generally too weak to be observed for hydrogen. H atoms, therefore, have been neglected in all simulations.

Experiments were performed in a Vacuum Generators ESCALAB Mk II spectrometer modified for motorized sequential angle-scanning data acquisition,[10] and with a base pressure in the low 10^{-11} mbar region. Photoelectron spectra and diffraction patterns were measured using Mg $K\alpha$ ($h\nu=1253.4$ eV) radiation with the sample kept at room temperature. The overall energy resolution is approximately 1 eV. In order to deplete the W(110) crystal from C, it was annealed to 1500 K during 125 h under an O_2 partial pressure of 10^{-7} mbar. Subsequently the crystal was flashed to

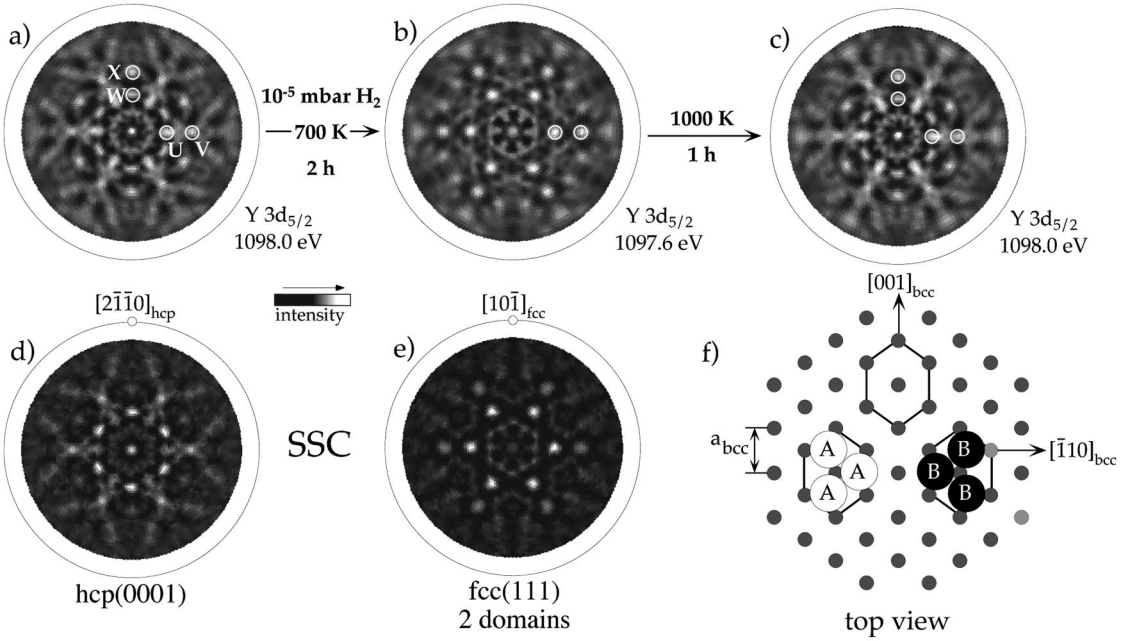

FIG. 1. Stereographic projection of experimental and calculated (SSC) Y $3d_{5/2}$ intensities. All patterns are oriented with the $[001]_{bcc}$ direction of the underlying W(110) crystal pointing to the top. Labels are explained in the text. (a) Y film as deposited. (b) Y film after H loading. (c) Y film after H unloading. (d) Calculation including Y atoms in eight layers of an (0001) oriented hcp cluster. (e) Calculation including Y atoms in eight layers of two fcc(111) clusters rotated by 180° with respect to each other. (f) Two possibilities (*A*, *B*) for closed-packed metal layers to start the stacking sequence on a quasihexagonal bcc(110) surface.

2500 K.[15] As a result, no C or O contaminations could be detected with x-ray photoelectron spectroscopy (XPS) and low-energy electron diffraction (LEED) displayed well-defined and sharp (1×1) spots indicating a well ordered surface. High purity Y (99.99%) was evaporated from a liquid-nitrogen-cooled electron-bombardment evaporation cell at pressures never exceeding 7×10^{-11} mbar and with the W(110) crystal held at 600 K. The thickness of all films was 200 Å as measured with a water-cooled quartz microbalance. After deposition, the W(110) signals were no longer visible and no O contamination could be detected with XPS. Due to the residual gas the O contamination level of both Y and Y hydride films increased by 0.2% per hour (cross-section corrected O 1*s* to Y 3*d* intensity ratio). Measuring times were chosen such that contamination remained below 1%.

Figures 1(a)–1(c) display the sequence of experiments starting with the clean Y film [Fig. 1(a)] being loaded with H [Fig. 1(b)] and unloaded again [Fig. 1(c)]. XPD from the Y film as deposited [Fig. 1(a)] reveals sixfold symmetry with a flowerlike design in the center and prominent maxima at $\Theta\approx34°$ (label *U*), $\Theta\approx52°$ (label *V*), $\Theta\approx34°$ (label *W*), and $\Theta\approx50°$ (label *X*). An SSC calculation including Y atoms in eight layers of an hcp(0001) oriented cluster [Fig. 1(d)] fits nicely with the experimental diffractogram [Fig. 1(a)]. Though still sixfold symmetric, exposure of the Y films to a H_2 partial pressure of 10^{-5} mbar (700 K during 2 h) induces drastic changes in the Y $3d_{5/2}$ diffractogram [Fig. 1(b)]. The flowerlike design in the center of the diffractogram becomes wheellike. Moreover, only maxima at $\Theta\approx34°$ (label *U*) and $\Theta\approx56°$ (label *V*) remain. The experiment is very well reproduced by an SSC calculation using eight layers of two equally populated fcc(111) domains rotated by 180° with respect to each other [Fig. 1(e)]. The fcc structure reveals the β phase.[1] Note that fcc(111) oriented Y dihydride films can also be produced by depositing Y under a H_2 partial pressure of 10^{-6} mbar.[16] Reversibility towards the α phase is achieved by heating the dihydride film to 1000 K during 1 h [Fig. 1(c)].

It is the change in the stacking sequence between the hcp ($ABAB\ldots$) and the fcc ($ABCABC\ldots$) phase that accounts for the disappearance of maxima caused by scattering events within next-nearest neighboring planes (labels *W*, *X*) when going from hcp [Fig. 1(a)] to fcc [Fig. 1(b)]. Except for the slight H-induced expansion of the Y lattice the lateral arrangement of Y atoms on the hcp(0001) surface is the same as that on fcc(111) surfaces. Therefore, a simple kinematic LEED pattern analysis would not provide conclusive information on the α to β phase transformation. However, the high definition of the LEED spots during H up- and unloading is indicative of the retention of long-range order. Maintenance and identification of short-range order is demonstrated by the well defined XPD patterns. Therefore, no loss of crystallinity occurred during these structural transformations. Moreover, both of these factors are consistent with the diffusionless translation of closed-packed Y planes, which is the mechanism behind *martensitic* transitions.[17] The formation of different domains is known to occur during *martensitic* transformations, accounting for the observation of two fcc(111) orientations rotated by 180° with respect to each other after H loading [Fig. 1(b)]. In the case of direct Y dihydride growth, when evaporating Y under H_2 partial pressure, two fcc(111) domains may be induced at the W-Y interface. Due to the quasihexagonality of the bcc(110) surface, closed-packed Y layers can start stacking either in the *A* or *B* orientation [Fig. 1(f)]. For the fcc case this results in two (111) oriented domains rotated by 180° with respect to each other. Finally, our XPD results show that both Y and Y

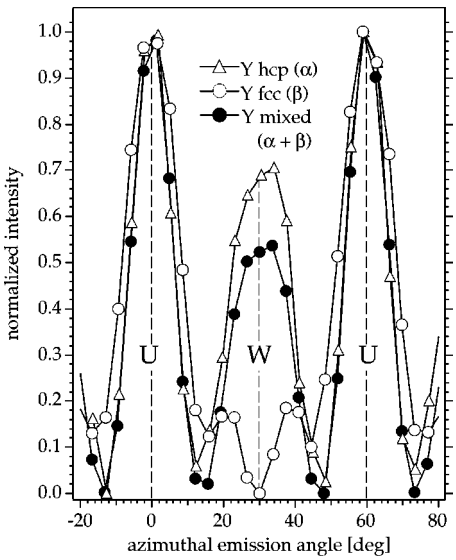

FIG. 2. Azimuthal scans at a polar angle of $\Theta = 34°$ illustrating the H-induced α to β phase transition. (△) Y film as deposited. (○) $YH_{1.8}$ film. (●) Y film in the two-phase regime.

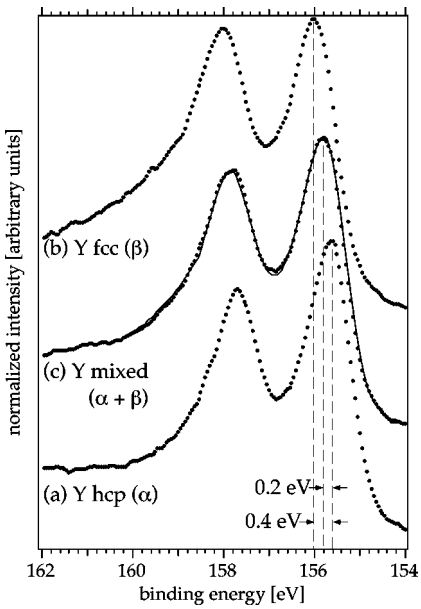

FIG. 3. XPS spectra illustrating peak positions and line shape of the Y 3*d* doublet during the H-induced α to β phase transition. (a) Y film as deposited. (b) $YH_{1.8}$ film. (c) Y film in the two-phase regime. The solid curve is the best fit to spectrum (c) (see text).

dihydride films grown on W(110) follow the so-called Nishiama-Wassermann orientation,[18] where most densely packed metal rows ($[2\bar{1}10]_{hcp}$, $[\bar{1}01]_{fcc}$) are parallel to the $[001]_{bcc}$ axis of the bcc(110) substrate [Figs. 1(d)–1(f)].

The α phase is a solid solution where the hydrogen atoms are distributed statistically in the tetrahedral interstices of the hcp Y lattice. As soon as the α phase is saturated ($\approx$0.2 H/Y),[1] with increasing H concentration, the system crosses into the two-phase ($\alpha+\beta$) regime until the saturated α phase has been completely converted to the β phase. The equilibrium pressure at the isothermal plateau of Y dihydride is very low (10^{-6} mbar at 800 K),[1] however, further hydrogen uptake needs much higher pressures than used in our experiments. Therefore, the H concentration of the dihydride film discussed in this study [Fig. 1(b)] corresponds to the lower boundary of the pure β phase, i.e., 1.8 H/Y. In the following we discuss the case of a Y film in the two-phase regime. This is done by means of azimuthal scans across the relevant forward focusing maxima (labels *U*, *W* in Fig. 1) and XPS core-level shift and line-shape analysis.

Figure 2 displays azimuthal cuts through the maxima labeled *U* and *W* (Fig. 1), respectively. The photoelectron intensities from each cut are normalized between 0 and 1. While the open triangles result from a cut through Fig. 1(a) or Fig. 1(c), open circles display the equivalent azimuthal scan through the Y dihydride film [Fig. 1(b)]. The curve with the black dots (its XPD pattern is not shown) is characteristic for a Y hydride film in the two-phase regime. By means of the *W*/*U* intensity ratio, linearly interpolating between the hcp and fcc structure, the population of the two phases can be estimated. For the mixed phase (black dots) we find that 24% of the Y atoms populate the β phase.

Figure 3 shows the photoemission intensity in the region of the XPS Y 3*d* doublet as a function of electron binding energy. Compared to the spectrum taken from the hydrogen free Y film [Fig. 3(a)], after H loading the Y 3*d* doublet is shifted by 0.4 eV towards higher binding energies [Fig. 3(b)]. Moreover, due to an intense high-binding-energy tail the linewidth is much larger. The change in chemical environment is necessarily due to hydride formation, since for both experiments the O contamination was below 0.5%. A shift of 0.4 eV is comparable to bulk values of Y dihydride.[6,7] Therefore, our interpretation of the XPD pattern of Fig. 1(b) in terms of a single-crystalline Y dihydride film is confirmed. In the two-phase regime the Y 3*d* doublet is shifted by 0.2 eV only [Fig. 3(c)], and its linewidth is not as broad as for the dihydride.

Since XPD very directly allows for a simple linear combination of the hcp and fcc structures the question arises whether this is also the case for the core-level spectra (Fig. 3). It turns out that a simple linear combination of (a) and (b) does not fit (c): neither the width nor the intensity ratio of the spin orbit split Y 3*d* is reproduced. The situation is more subtle. Very good coincidence in peak positions and intensity ratio is only achieved when the pure metal spectrum used for the linear combination is first shifted towards higher binding energies and then linearly combined with the dihydride spectra. In the present case the best fit (solid curve in Fig. 3) is achieved with $\Delta E = 0.08$ eV and 26% of the dihydride phase in good agreement with the XPD results.

This procedure can be explained within the following model. As the H concentration increases in the α phase the line shape of the Y 3*d* doublet is not modified. Due to charge transfer from Y to H, however, its peak position shifts toward higher binding energy. In the pure α phase (0 to 0.2 H/Y) the concentration is therefore estimated via the chemical shift of the Y 3*d* doublet. In the two-phase regime spectra can be reproduced by a linear combination of the spectrum from the saturated pure α phase with the one obtained from the Y film at the lower boundary of the pure β phase [Fig. 3(b)]. From the resulting coefficients the H concentration can be calculated easily. In the case of the two-phase Y film discussed here we find a concentration of $\approx$0.6 H/Y. In general, this model allows to evaluate H concentrations up to

1.8 H/Y (lower boundary of the pure β phase) by means of photoelectron spectra of the Y $3d$ doublet. Since already low O contaminations induce substantial changes in the shape and energy position of the Y $3d$ doublet,[16] this method requires very clean samples. Moreover, estimated concentrations are based on the literature values of the critical H concentration for both the saturated α phase (0.2 H/Y) as well as for the low boundary of the pure β phase (1.8 H/Y). The values are rather widely scattered depending on the material purity.[1] However, this spectroscopic *in situ* method is very promising in that it may also be applied to the β to γ phase transition as well as to other RE hydrides.

In summary, we have grown well ordered single-crystalline hcp(0001) Y films on a W(110) crystal. Reversible hydrogen loading up to the fcc dihydride phase was achieved under a H_2 partial pressure of 1×10^{-5} mbar. Two fcc(111) domains rotated by 180° with respect to each other are observed. No loss of crystallinity occurred during the reversible, H-induced *martensitic* transformations of the Y lattice, a fundamental condition to acquire accurate band-structure data via ARUPS experiments.[16] A model for H concentration estimation, based on line shape and peak position analysis of the Y $3d$ core level, is proposed. Consistent with the XPS analysis, XPD offers the possibility to directly determine the phase population in the two-phase regime. XPD turned out to be a suitable method to observe the behavior, in real space and near the surface, of the Y lattice during H loading. We would like to point out that the application of XPD is by no means limited to the α to β phase transition in Y. Phase transitions in other RE's are expected to be similarly well imaged by this technique.

We profited from stimulating discussions with A. Züttel and J. Osterwalder. Skillful technical assistance was provided by F. Bourqui, Ch. Neururer, E. Mooser, and O. Raetzo. This project has been supported by the Fonds National Suisse pour la Recherche Scientifique and the EU HCM Project No. CHRX-CT93-0371.

[1] P. Vajda, in *Handbook on the Physics and Chemistry of Rare Earths*, edited by K. A. Gschneider and L. Eyring (Elsevier, Amsterdam, 1995), Vol. 20.

[2] J. N. Huiberts, R. Griessen, J. H. Rector, R. J. Wijngaarden, J. P. Dekker, D. G. de Groot, and N. J. Koeman, Nature (London) **380**, 231 (1996).

[3] T. J. Udovic, Q. Huang, and J. J. Rush, J. Phys. Chem. Solids **57**, 423 (1996).

[4] J. H. Weaver, D. T. Peterson, and R. L. Benbow, Phys. Rev. B **20**, 5301 (1979).

[5] J. H. Weaver, D. T. Peterson, R. A. Butera, and A. Fujimori, Phys. Rev. B **32**, 3562 (1985).

[6] A. Fujimori and L. Schlapbach, J. Phys. C **17**, 341 (1984).

[7] J. Osterwalder, Z. Phys. B **61**, 113 (1985).

[8] A. Remhof, G. Song, K. Theis-Bröhl, and H. Zabel, Phys. Rev. B **56**, R2897 (1997).

[9] C. S. Fadly, in *Synchrotron Radiation Research: Advances in Surface Science*, edited by R. Z. Bachrach (Plenum, New York, 1990), Vol. 1.

[10] J. Osterwalder *et al.*, Surf. Sci. **331-333**, 1002 (1995).

[11] R. Fasel, P. Aebi, R. G. Agostino, D. Naumović, J. Osterwalder, A. Santaniello, and L. Schlapbach, Phys. Rev. Lett. **76**, 4733 (1996).

[12] Ph. Aebi, R. Fasel, D. Naumovic, J. Hayoz, Th. Pillo, M. Bovet, R. G. Agostino, L. Patthey, F. P. Gil, H. Berger, T. J. Kreutz, J. Osterwalder, and L. Schlapbach, Surf. Sci. **402**, 614 (1998).

[13] J. Hayoz, D. Naumović, R. Fasel, P. Aebi, and L. Schlapbach, Surf. Sci. **373**, 153 (1997).

[14] D. Gregory and M. Fink, At. Data Nucl. Data Tables **14**, 39 (1974).

[15] S. Sarbach, Diploma thesis, University of Fribourg, Switzerland, 1998.

[16] J. Hayoz *et al.* (unpublished).

[17] J. W. Christian, *The Theory of Transformation in Metals and Alloys*, 2nd ed. (Pergamon, Oxford, 1981).

[18] L. A. Bruce and H. Jaegger, Philos. Mag. A **38**, 223 (1978).